pISSN 1598-2033
eISSN 2233-5706

Journal of the Korea Institute of Building Construction, Vol. 14, No. 1
http://dx.doi.org/10.5345/JKIBC.2014.14.1.068

www.jkibc.org

Formation of Hydroxyapatite in Portland Cement Paste

Chung, Chul-Woo Lee, Jae-Yong Kim, Ji-Hyun*

Department of Architectural Engineering, Pukyong National University, Nam-Gu, Busan, 608-739, S-Korea

Abstract

In order to increase the integrity of the wellbore which is used to prevent the leakage of supercritical CO_2, it is necessary to develop a concrete that is strongly resistant to carbonation. In an environment where the concentration of CO_2 is exceptionally high, Ca^{2+} ion concentration in pore solution of Portland cement concrete will drop significantly due to the rapid consumption of calcium hydroxide, which decreases the stability of the calcium silicate hydrate. In this research, calcium phosphates were used to modify Portland cement system in order to produce hydroxyapatite, a hydration product that is strongly resistant to carbonation under such an environment. According to the experimental results, calcium phosphates reacted with Portland cement to form hydroxyapatite. The formation of hydroxyapatite was verified using X-ray diffraction analyses with selective extraction techniques. When using dicalcium phosphate dihydrate and tricalcium phosphate, the 28-day compressive strength was lower than that of plain cement paste. However, the specimen with monocalcium phosphate monohydrate showed equivalent strength to that of plain cement paste.

Keywords : portland cement, calcium phosphate, hydroxyapatite, geologic sequestration, carbon dioxide

1. Introduction

Carbonation is a natural process that forms carbonate precipitates through a reaction with atmospheric CO_2 in the presence of moisture[1]. In Portland cement concrete, the main reaction products are calcium silicate hydrate (C-S-H) and calcium hydroxide[1,2], and the carbonation process takes place by consuming calcium hydroxide in the concrete. The formation of calcite first occurs at the outer surface of the concrete. The outer calcite layer (carbonation front) becomes protective against the permeation of CO_2 and moisture (also other aggressive ionic species), and hinders carbonation[3].

Received : October 15, 2013
Revision received :
Accepted : November 25, 2013
* Corresponding author : Kim, Ji-Hyun
[Tel: 82-51-629-6089, E-mail: ster-h@hanmail.net]

When Portland cement concrete is used for the geologic sequestration of CO_2, it will be in contact with supercritical CO_2 that is dissolved in the aqueous phase. As a result, carbonic acid attacks the cement matrix. Portlandite [$Ca(OH)_2$(s)] is dissolved by carbonic acid as the carbonated water diffuses into the cement matrix, resulting in the increased leaching of Ca^{2+} out of the cement matrix and an increase in the porosity. Further degradation by carbonic acid also causes the dissolution of calcite, which is called bicarbonation reaction[4]. These continuous reaction processes will significantly drop the stability of the calcium silicate hydrate (C-S-H), causing decalcification of C-S-H that forms hydrous silica[3]. Decalcification of C-S-H causes severe degradation in concrete because C-S-H is the main structural component in concrete.

The degree of cement degradation caused by supercritical CO_2 has been reported to be variable due to the wide variation in laboratory experimental conditions such as temperature, pressure, and cement

curing[5]. A number of studies have shown that wellbore cement is susceptible to CO_2 attack, leading to rapid degradation[6,7], whereas other studies indicate that CO_2 penetration and reaction with cement is limited[5,8], and the long-term performance of wellbore cement in a CO_2-enhanced oil recovery field was good, providing an effective barrier to significant fluid flow for decades[9,10]. Despite numerous previous studies reporting the geochemical and mineralogical alteration of well cement by CO_2 under geologic sequestration conditions[5,8,11], the rate of Portland cement degradation and long-term integrity of wellbore cement material is still in question and under debate.

Considering the relations on solubility of materials, phosphate-based materials usually have lower solubility products than calcite. Therefore, the formation of stable calcium phosphate hydration products in Portland cement can be a good candidate to minimize the damage associated with carbonation from supercritical CO_2. In the hydration of reactive calcium phosphate, the reaction kinetic is quite simple: when calcium phosphates (monocalcium, dicalcium, tricalcium phosphates, etc.) are in contact with water, hydroxyapatite [$Ca_5 \cdot (PO_4)_3 \cdot OH$] and phosphoric acid[12] are produced. In Portland cement system, the phosphoric acid will be neutralized due to the presence of portlandite. Since the reaction product, hydroxyapatite, is known as one of the most stable phases that is present on earth, our approach to produce hydroxyapatite in Portland cement concrete is likely to provide durability of concrete that is exposed to the supercritical CO_2 environment.

The objective of this work is to find an alternative way to minimize the carbonation of concrete used for geologic sequestration of CO_2. It should be noted that there is little experimental work done to make such modification. In this work, the formation of hydroxyapatite in Portland cement paste using three different forms of calcium phosphates was verified using XRD analyses. The 28-day compressive strength was also compared to provide basic information.

2. Experimental Procedures

2.1 Sample preparation

Table 1 shows the mixture proportions of cement pastes. ASTM type I Portland cement was used to prepare plain cement paste. The Portland cement was modified using reagent grade calcium phosphates. Calcium phosphates used in this research included monocalcium phosphate monohydrate, $Ca(H_2PO_4)_2 \cdot H_2O$ (Junsei Chemical Co., Ltd. Japan), dicalcium phosphate dihydrate (Brushite), $CaHPO_4 \cdot 2H_2O$ (Katayama Chemical Co., Ltd. Japan), and tricalcium phosphate, $Ca_3(PO_4)_2$ (Junsei Chemical Co., Ltd. Japan). Distilled water was used for the experiments, and the water to solid ratio (w/s) was set at 0.45. To maintain the same water to solid ratio, the amount of water in calcium phosphates (chemically bound H_2O) was considered when calculating the total amount of water used for the mix.

Plain cement pastes of w/s 0.45 were prepared by mixing 1200 g cement and 540 g distilled water in planetary paddle mixer (Heungjin Testing Machine Co., Ltd. Korea, HJ-1150). The mixing procedure basically followed the procedure given in ASTM C 305, Standard Practice for Mechanical Mixing of Hydraulic Cement Pastes and Mortars of Plastic Consistency, the cement paste mix part. Paste was first mixed for 30 seconds at the lower speed level (62rpm), and the mixer was stopped for 30 to 60 seconds in order to scrape off cement paste adhering to the side of the mixing bowl. As soon as scraping was finished, the paste was mixed for 90 seconds at the fastest speed level (125rpm).

As soon as the testing specimens were mixed, they were placed in the mortar cube mold (50mm×50mm

×50mm) for curing. The top portion of the cube mold was covered using plastic wrap to prevent the evaporation of moisture. The cube mold was removed at 3 days after mixing for further curing in ambient air and also in lime saturated solution. Total curing time was 28 days.

Table 1. Mix proportions of the cement pastes

Specimen	Source of phosphate	Weight (g)		
		Water	Cement	Phosphate
Plain	-	540	1200	-
CP1	$Ca(H_2PO_4)_2 \cdot H_2O$	530.8	1080	129.2
CP2	$CaHPO_4 \cdot 2H_2O$	508.2	1080	151.8
CP3	$Ca_3(PO_4)_2$	540	1080	120

*Note that CP1 incorporates monocalcium phosphate monohydrate, CP2 incorporates dicalcium phosphate dehydrate, and CP3 incorporates tricalcium phosphate in the Portland cement paste.

2.2 XRD

Both the unhydrated cement and the hydrated cement pastes were analyzed. For the phase compositions of 28-day hydrated cement pastes, chunks of paste specimens were ground using an agate mortar and pestle. The dry powdered specimens were then packed into the sample container, and the sample container was placed in the X-ray diffractometer (Rigaku Co., Ltd. Japan, Ultima IV) with Cu Kα radiation. The scanned 2-theta angle (2θ) was from 5° to 70° with a step size of 0.02° and a dwell time of 1 sec. The working voltage was 40 kV and the electric current was 40 mA.

2.2.1 Salycylic Acid/Methanol extraction

Salicylic Acid/Methanol (SAM) extraction was used to remove calcium silicates. The purpose was to facilitate the XRD analysis of C_3A (aluminate), C_4AF (ferrite), calcium sulfate, and hydroxyapatite, if present. The sample, 5 g of unhydrated cement or hydrated cement pastes, was added to a solution containing 20 g of salicylic acid in 300 ml methanol. The mixture was stirred for 2 hours, and the suspension was vacuum filtered using a Buchner funnel and a filter paper. The residue was washed with methanol and dried in a 60°C oven until XRD analysis.

2.2.2 KOH/sugar extraction

Potassium hydroxide/sugar (KOH/sugar) extraction was used to dissolve C_3A and C_4AF, leaving a residue of calcium silicates, carbonates, and minor phases. The purpose was to facilitate the XRD analysis of C_3S, C_2S, and possibly hydroxyapatite. Extraction solution was prepared using 30 g of KOH and 30 g of sucrose in 300 ml of deionized water. The sample, 9 g of hydrated cement paste, was added to the extraction solution kept at a temperature of 95°C and stirred for a minute. The suspension was vacuum filtered using a Buchner funnel and a filter paper. The residue was washed with 50 ml of water followed by 100 ml of methanol and dried in a 60°C oven until XRD analysis.

2.3 Compressive strength

The 28-day compressive strength measurements were performed using a universal testing machine (Shimadzu Co., Ltd. Japan, UH-F100A). The loading rate of the specimens was fixed at 3mm/min.

3. Results

3.1 XRD

3.1.1 Unhydrated cement

Figure 1 shows the XRD patterns of unhydrated cement paste. The upper part of the XRD pattern is SAM extracted cement, and the lower part of the XRD pattern is the cement as received (unhydrated). The observed phases in unhydrated cement are also summarized in Table 2. Unhydrated cement (unextracted, lower XRD pattern in Figure 1) shows the presence of C_3S, C_2S, C_4AF, gypsum, periclase,

and calcite. Since the identification of C_3A in cement was difficult, SAM extraction was performed, and the orthorhombic C_3A was observed from SAM extracted cement (upper XRD pattern). The SAM extracted XRD pattern also confirmed the presence of C_4AF, gypsum, calcite, bassanite (calcium sulfate hemihydrate), and periclase. Clear indication of syngenite (2θ angles at 9.31°, 15.51°, 18.71°, 19.18°, 19.73°, etc.), although its X-ray intensity was small, was identified. Syngenite is a reaction product between calcium langbeinite (potassium calcium sulfate) and water or a reaction product between arcanite (potassium sulfate), calcium sulfate (generally in the form of gypsum), and water [13]. However, calcium langbeinite and arcanite was not clearly identified from the XRD pattern of unextracted cement due to its minor trace quantity, and neither calcium langbeinite nor arcanite were observed in the SAM extracted sample. The best assumption is that some vapor condensation associated with slow vacuum filtration during humid conditions (a typical weather condition in summer of Busan) occurred during SAM extraction, and caused a secondary reaction to form syngenite. It is also possible that the water present in methanol could have formed such a hydration product.

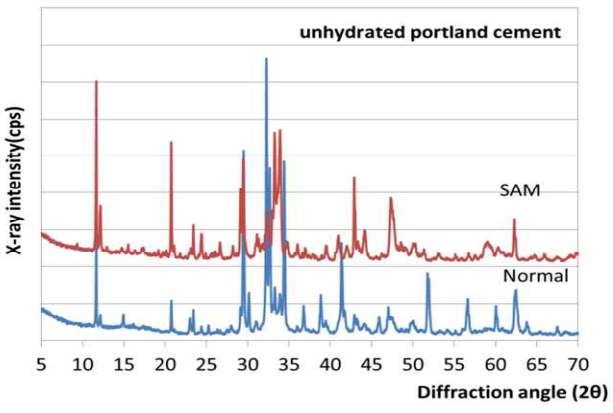

Figure 1. XRD pattern of unhydrated cement before and after SAM extraction

Table 2. Phase identification of Portland cement

PDF ID	Chemical composition	Mineral name
32-0150	$Ca_3Al_2O_6$	Orthorhombic C_3A
30-0226	$Ca_2(Al,Fe)_2O_5$	Brownmillerite (C_4AF)
05-0586	$CaCO_3$	Calcite
04-0829	MgO	Periclase
33-0311	$CaSO_4 \cdot 2H_2O$	Gypsum
13-0272	$Ca_{54}MgAl_2Si_{16}O_{90}$	Impure C_3S, Alite
49-0442	Ca_3SiO_5	C_3S
33-0302	Ca_2SiO_4	Larnite(belite),C_2S
41-0224	$CaSO_4 \cdot 0.5H_2O$	Bassanite (calcium sulfate hemihydrate)
28-0739	$K_2Ca(SO_4)_2 \cdot 2H_2O$	Syngenite

*Note that syngenite was formed during SAM extraction.

3.1.2 Hydrated cement

The XRD patterns of hydrated cement pastes are shown in Figure 2. As in Figure 1, the lower XRD pattern is for hydrated cement paste, and upper XRD pattern is for SAM extracted cement paste. According to Figure 2 (unextracted, lower XRD pattern), the dominant XRD peaks are associated with portlandite (calcium hydroxide; at 18.05°, 28.70°, 34.11°, 36.56°, 47.13°, 50.84°, 54.39°, etc.). Other major peaks are associated with ettringite. Since both portlandite and ettringite are crystalline, they can be easily detected by XRD and seem to dominate other peaks although their quantity is not as much. Carbonate AFm peaks are also observed at 10.78° (hemicarbonate) and 11.67° (monocarbonate). Some amount of C_3S, C_2S, and C_4AF were still observed, indicating that they were not completely hydrated. Determination of C-S-H from XRD pattern was difficult due to its amorphous characteristic.

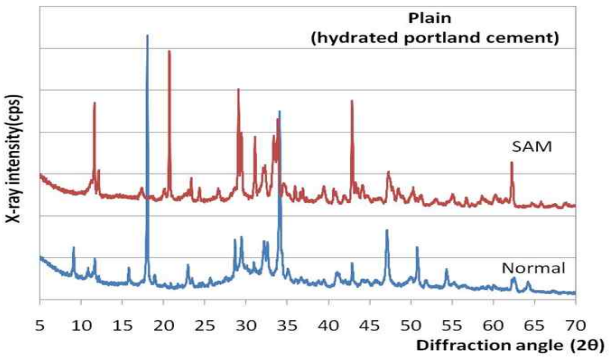

Figure 2. XRD pattern of plain cement paste before and after SAM extraction

Table 3. Phase identification of hydrated Portland cement

PDF ID	Chemical composition	Mineral name
32-0150	$Ca_3Al_2O_6$	Orthorhombic C_3A
30-0226	$Ca_2(Al,Fe)_2O_5$	Brownmillerite (C_4AF)
05-0586	$CaCO_3$	Calcite
04-0829	MgO	Periclase
33-0311	$CaSO_4 \cdot 2H_2O$	Gypsum
78-2050	$Ca_8Al_4(OH)_{24}(CO_3)Cl_2(H_2O)_{1.6}(H_2O)_8$	Hydrocalumite
13-0272	$Ca_{54}MgAl_2Si_{16}O_{90}$	Impure C_3S, Alite
33-0302	Ca_2SiO_4	Larnite (belite), C_2S
44-1451	$Ca_6Al_2(SO_4)_3(OH)_{12} \cdot 26H_2O$	Ettringite
44-1481	$Ca(OH)_2$	Portlandite
36-0129	$Ca_8Al_4O_{14}CO_3 \cdot 24H_2O$	Hemicarbonate
41-0219	$Ca_4Al_2O_6CO_3 \cdot 11H_2O$	monocarbonate

SAM extracted the XRD pattern (upper XRD part of Figure 2) of hydrated cement paste showed orthorhombic C_3A. It is interesting to see C_3A after 28 days of hydration. A fairly high gypsum peak intensity was also observed from the SAM extracted XRD pattern. The reason why C_3A is not completely hydrated is still unclear at this moment. It also seems that hydrocalumite (naturally occurring AFm phase, the coexistence of Cl^- and CO_3^{2-} between calcium aluminate layers; layered double hydroxide) exists in the SAM extracted paste sample.

However, it should be noted that the ettringite and other carbonate AFm phases disappeared after SAM extraction. Therefore, there is no reason to consider that hydrocalumite was not removed from SAM extraction. Similarly to the case of syngenite formation from SAM extracted unhydrated cement, there was some amount of unreacted C_3A in the hydrated cement paste, and it was reacted with water (associated either with the vapor condensation during slow speed vacuum filtration or with the methanol) to form hydrocalumite. Table 3 summarizes the observed phases from the hydrated cement paste.

3.1.3 Hydrated cement with calcium phosphates

The XRD patterns of hydrated cement pastes with and without calcium phosphates are shown in Figure 3. Table 4 also summarizes the identified phases from hydrated cement paste with calcium phosphates. According to Figure 3, the XRD patterns of cement paste using various types of calcium phosphates were very similar to each other.

Table 4. Phase identification of hydrated Portland cement modified using calcium phosphates

PDF ID	Chemical composition	Mineral name
32-0150	$Ca_3Al_2O_6$	Orthorhombic C_3A
30-0226	$Ca_2(Al,Fe)_2O_5$	Brownmillerite (C_4AF)
05-0586	$CaCO_3$	Calcite
04-0829	MgO	Periclase
33-0311	$CaSO_4 \cdot 2H_2O$	Gypsum
09-0432	$Ca_5(PO_4)_3OH$	Hydroxyapatite
78-2050	$Ca_8Al_4(OH)_{24}(CO_3)Cl_2(H_2O)_{1.6}(H_2O)_8$	Hydrocalumite
13-0272	$Ca_{54}MgAl_2Si_{16}O_{90}$	Impure C_3S, Alite
33-0302	Ca_2SiO_4	Larnite (belite), C_2S
44-1451	$Ca_6Al_2(SO_4)_3(OH)_{12} \cdot 26H_2O$	Ettringite
44-1481	$Ca(OH)_2$	Portlandite
36-0129	$Ca_8Al_4O_{14}CO_3 \cdot 24H_2O$	Hemicarbonate
41-0219	$Ca_4Al_2O_6CO_3 \cdot 11H_2O$	monocarbonate

* Note that all the hydrated cement pastes using monocalcium, dicalcium, and tricalcium phosphates showed the same hydration products. No clear differences were observed from the phase identification.

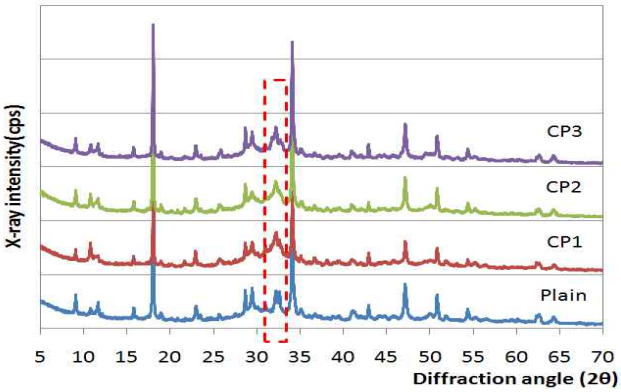

Figure 3. XRD patterns of hydrated cement pastes with and without calcium phosphates

XRD patterns between plain cement paste and cement pastes with various calcium phosphates are very similar, but the difference was observed between 31° and 33° 2θ angle (indicated as the dotted rectangle in Figure 3). XRD peak at this range became wider when calcium phosphates were added. The widened XRD peak can be explained either by multiple

peak responses (each of the individual peaks are closely located) over a range of angles or by the amorphous nature of the phase. However, the range of 2θ angle between 31° and 33° also includes the main peaks of C_3S, C_2S, and C_3A. Since the main XRD peak of hydroxyapatite is also located in this area (main peak at 31.77°, 32.20°, and 32.90°), it was difficult to verify the formation of hydroxyapatite from the XRD pattern. Thus, SAM extraction was applied to hydrated cement paste samples in order to remove calcium silicates and other hydration phases, assuming that hydroxyapatite does not dissolve during SAM extraction.

The SAM-extracted XRD patterns of hydrated cement pastes with and without calcium phosphate are presented in Figure 4. The XRD peaks of CP series specimens between 31° and 33° are still wide after SAM extraction. The plain cement paste does not show such a wide XRD peak. It should be noted that the wide XRD peak can be associated with a mixture of C_3A, C_4AF, gypsum, and hydroxyapatite peaks, so the analyses of the results are still cumbersome.

According to Figure 4, plain cement paste showed a maximum XRD peak at 32.12°, and seems to be associated with unreacted brownmillerite (C_4AF), but in cement pastes with calcium phosphates the maximum of the XRD peak was much wider. Although it is difficult to verify the presence of hydroxyapatite due to the peak overlaps of C_3A, gypsum, and C_4AF, the widened peak at 31° to 33° and the peak widening (survived after SAM extraction) can be reasonably explained considering the main peak response of hydroxyapatite (main peaks at 31.77°, 32.20°, and 32.90°).

Figure 5 shows XRD patterns of the KOH/sugar extracted samples. After KOH/sugar extraction, the widened peak at 31° to 33° was still observed in cement pastes with calcium phosphates, whereas such peak was not clearly observed from plain cement paste. In plain cement paste, the peak at 31.12° was gypsum. Two other peaks (at 32.14 and at 32.59°) were unreacted C_2S (larnite). Since KOH/sugar extraction removes C_3A and C_4AF, the results verify that this widened peak shown in Figure 5 from cement pastes with calcium phosphates came from interaction between Portland cement and calcium phosphates.

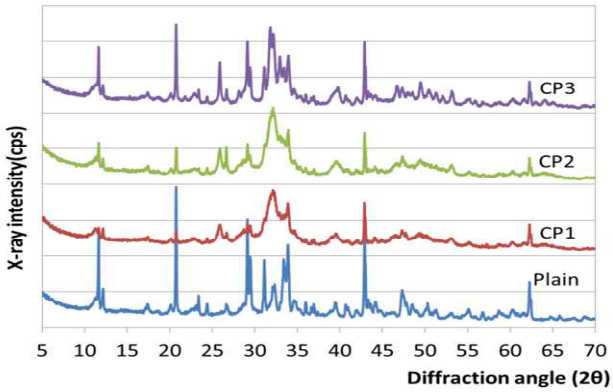

Figure 4. SAM-extracted XRD patterns of hydrated cement pastes with and without calcium phosphates

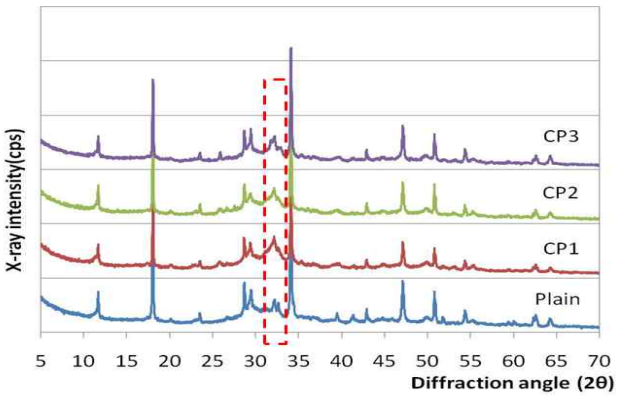

Figure 5. KOH sugar extracted XRD patterns of hydrated cement pastes with and without calcium phosphates

3.1.4 Differences in curing method

As noted earlier, the samples were cured in both ambient air and lime saturated solution. This was to determine whether there was any abnormal behavior in phase composition (mineralogy) using calcium phosphates when it was cured in different conditions. According to the XRD analysis (although not shown in the Figures), it was found that there was no difference in the mineralogy of the hydrated

material, regardless of the curing method. Since XRD results of the samples cured in ambient air could represent the mineralogy of both samples, only the results from ambient air curing were presented in sections 3.2.2 and 3.2.3.

3.2 Compressive strength

The 28-day compressive strengths of cement paste are shown in Figure 5. According to Figure 5, it was shown that plain cement paste had the highest compressive strength in general. Cement paste with monocalcium phosphate monohydrate (CP1) showed comparable compressive strength to the plain cement paste when the results from both curing conditions were averaged (lower in ambient air, but higher in lime saturated solution). However, the addition of both dicalcium phosphate dihydrate (CP2) and tricalcium phosphate (CP3) showed a clear reduction in compressive strength compared to that of plain cement paste.

3.3 Compressive strength

Since it was shown that the mineral compositions of CP series specimens are the same, the differences in compressive strength could be better related to the physical properties such as porosity and microstructural development in early age associated with the degree of hydration with each calcium phosphate sources.

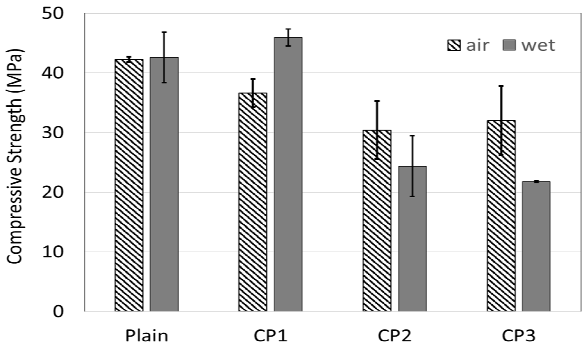

Figure 5. 28-day compressive strength of cement pastes, with and without calcium phosphates

4. Discussion

The objective of this work is to determine whether durable hydroxyapatite phase can be formed in Portland cement system. XRD analysis was used for this verification, and to facilitate the XRD analysis both SAM and KOH/sugar extraction were applied. The summaries of the XRD analyses are as follows:

1) The widened peak between 31° and 33° that survived after SAM and KOH/sugar extraction should not be related to C_3S, C_2S, C_3A, C_4AF, ettringite, AFm, and portlandite.
2) The center of the widened peak is very close to the main peak response of crystalline hydroxyapatite peak.

The summary of XRD analyses indicates that it is very likely for hydroxyapatite to be formed in the Portland cement system when various calcium phosphates were added. However, it should be noted that the formation of hydroxyapatite did not always lead to an increase in compressive strength. Many questions still remain regarding why compressive strength was lower when dicalcium phosphate dihydrate and tricalcium phosphate were added to Portland cement. Mostly, the difference in strength should be related to the differences in microstructural development, but there is not enough information available in the current literature. At least, the lower compressive strength should be related to the increase in porosity, and therefore it is difficult to argue that the formation of hydroxyapatite in Portland cement cannot always lead to the increase in durability when it is exposed to an environment with supercritical CO_2. The key is to produce hydroxyapatite with a reduced porosity.

It should be noted that the findings of this study are just the first step toward achieving the goal of developing a durable concrete formulation for the geologic sequestration of CO_2. To develop a better

product for this specific purpose, it is necessary to understand the interaction between Portland cement with various phosphates. It is important to investigate the differences in early hydration kinetics, pH changes, changes in Ca^{2+} concentration in pore solution, delay in setting and hardening, the interaction between certain phosphates with Portland cement, and finally the degree of hydration in the Portland cement system.

5. Conclusions

Based on the results provided in this work, following conclusions can be drawn:

1) Hydroxyapatite can be formed in Portland cement paste when monocalcium phosphate monohydrate, dicalcium phosphate dihydrate, and tricalcium phosphate are added to the Portland cement paste.
2) The formation of hydroxyapatite did not always lead to an improvement in compressive strength. The compressive strength of cement paste with monocalcium phosphate was comparable to that of plain cement paste, but it became lower with the addition of dicalcium phosphate dihydrate, and tricalcium phosphate.

Acknowledgement

This work was supported by a Research Grant of Pukyong National University (2013Year) (C-D-2013-0382).

References

1. Mindess S, Young JF, Darwin D. Concrete. 2nd ed. Upper Saddle River (NJ): Prentice Hall; 2003. 644 p.
2. Mehta PK, Monteiro PJM. Concrete Microstructure, Properties, and Materials. 3rd ed. New York (NY); McGraw Hill; 2005. 659 p.
3. Taylor HFW. Cement Chemistry. 2nd ed. London (UK): Thomas Telford Services Ltd; 1997. 459 p.
4. Krupka KM, Cantrell KJ, McGrail BP. Thermodynamic Data for Geochemical Modeling of Carbonate Reactions Associated with CO_2 Sequestration-Literature Review. Richland (WA): Pacific Northwest National Laboratory; 2010. 135 p.
5. Kutchko BG, Strazisar BR, Lowry GV, Dzombak DA, Thaulow N. Rate of CO_2 attack on hydrated Class H well cement under geologic sequestration conditions. Environmental Science and Technology. 2008 August;42(16):6237-42.
6. Barlet-Gouédard V, Rimmelé G, Goffé B, Porcherie O. Mitigation strategies for the risk of CO_2 migration through wellbores. Proceedings of the IADC/SPE Drilling Conference; 2006 February 21-23; Miami (FL). Richardson (TX): Society of Petroleum Engineers; 2006. SPE 98924-MS.
7. Scherer GW, Celia MA, Prevost J-H, Bachu S, Bruant R, Duguid A, Fuller R, Gasda SE, Radonjic M, Vichit-Vadakan W. Leakage of CO_2 through abandoned wells: role of corrosion of cement, in: Thomas D, Benson S. (Ed.), CO_2 Capture Project Technical Results. Amsterdam (Netherlands): Elsevier; 2005. p. 827-48.
8. Kutchko BG, Strazisar BR, Dzombak DA, Lowry GV, Thaulow N. Degradation of well cement by CO_2 under geologic sequestration conditions. Environmental Science and Technology. 2007 July;41(13):4787-92.
9. Carey JW, Wigand M, Chipera SJ, WoldeGabriel G, Pawar R, Lichtner PC, Wehner SC, Raines MA, Guthrie GD. Analysis and performance of oil well cement with 30 years of CO_2 exposure from the SACROC Unit, West Texas, USA. International Journal of Greenhouse Gas Control. 2007 April;1(1):75-85.
10. Crow W, Carey JW, Gasda S, Williams DB, Celia M. Wellbore integrity analysis of a natural CO_2 producer. International Journal of Greenhouse Gas Control. 2010 March;4(2):186-97.
11. Kutchko BG, Strazisar BR, Huerta N, Lowry GV, Dzombak DA, Thaulow N. CO_2 Reaction with Hydrated Class H Well Cement under Geologic Sequestration Conditions: Effects of Flyash Admixtures. Environmental Science and Technology. 2009 May;43(10):3947-52.
12. Odler I. Special Inorganic Cements, 1st ed. London (UK): E&FN SPON; 2000. 395 p.
13. Chung CW, Lee JY. Premature Stiffening of Cement Paste Associated with AFm Formation. Journal of the Korea Institute of Building Construction. 2011 February;11(1):83-90.